



Published in final edited form as:

*J Cell Biochem.* 2016 March ; 117(3): 769–779. doi:10.1002/jcb.25362.

## Occludin Content Modulates Hydrogen Peroxide–Induced Increase in Renal Epithelial Paracellular Permeability

Danielle Janosevic<sup>1</sup>, Josephine Axis<sup>2</sup>, Robert L. Bacallao<sup>1</sup>, and Kurt Amsler<sup>2,\*</sup>

<sup>1</sup>Division of Nephrology, Department of Medicine, Indiana University School of Medicine, Indianapolis 46202, Indiana

<sup>2</sup>Department of Biomedical Sciences, NYIT College of Osteopathic Medicine, Old Westbury 11568, New York

### Abstract

The ability of hydrogen peroxide (H<sub>2</sub>O<sub>2</sub>) to increase paracellular permeability of renal epithelial cell monolayers was examined and the role of occludin in this regulation was investigated. H<sub>2</sub>O<sub>2</sub> treatment increased the paracellular movement of calcein, a marker for the leak pathway permeability, across monolayers of two renal epithelial cell lines, MDCK and LLC-PK<sub>1</sub>, in a concentration-dependent manner. At the same concentrations, H<sub>2</sub>O<sub>2</sub> did not alter transepithelial resistance (TER) nor increase cell death. The magnitude of the H<sub>2</sub>O<sub>2</sub>-induced increase in leak pathway permeability was inversely related to cellular occludin protein content. H<sub>2</sub>O<sub>2</sub> treatment did not produce any major change in total cellular content or Triton X-100-soluble or –insoluble fraction content of occludin protein. Occludin protein staining at the tight junction region was diminished following H<sub>2</sub>O<sub>2</sub> treatment. The most dramatic effect of H<sub>2</sub>O<sub>2</sub> was on the dynamic mobility of GFP-occludin into the tight junction region. H<sub>2</sub>O<sub>2</sub> treatment slowed lateral movement of GFP-occludin into the tight junction region but not on the apical membrane. Further, removal of the cytoplasmic C-terminal region of occludin protein eliminated the effect of H<sub>2</sub>O<sub>2</sub> on GFP-occludin lateral movement into the tight junction region. An increase in the mobile fraction of GFP-occludin was associated with a loss of response to H<sub>2</sub>O<sub>2</sub>. These data indicate that the H<sub>2</sub>O<sub>2</sub>-induced increase in renal epithelial cell paracellular permeability is mediated, at least in part, through occludin protein, possibly through a slowing of the rate of occludin movement into the tight junction region.

### Keywords

FRAP; HYDROGEN PEROXIDE; OCCLUDIN; RENAL EPITHELIAL CELL; TIGHT JUNCTION

---

Tight junctions are circumferential junctions joining adjacent epithelial cells at the apicolateral border. The tight junction forms the primary paracellular permeability barrier restricting the movement of solutes, water, toxins, and pathogens between epithelial cells

---

\*Correspondence to: Kurt Amsler, Department of Biomedical Sciences, NYIT College of Osteopathic Medicine, P.O.Box 8000, Old Westbury 11568, NY. kamsler@nyit.edu.

Conflict of Interest: The authors declare no conflict of interest.

across epithelial cell layers. It is a multiprotein complex comprised of membrane proteins, including claudins, occludin, and tricellulin, and multiple cytoplasmic proteins, including ZO-1, ZO-2, and cingulin (for reviews, see Shen et al., 2011; Szaszi and Amoozadeh, 2014). Paracellular permeability is divided into two pathways, the pore pathway characterized by the large capacity diffusion of small solutes and the leak pathway characterized by the small capacity diffusion of larger solutes.

Occludin protein has been suggested to be an important regulator of epithelial tight junction functional properties and their modulation by stimuli (see, e.g., Feldman et al., 2005; Rao, 2009; Cummins, 2012). Studies have demonstrated definitively a role for occludin protein in mediating baseline paracellular permeability of intestinal epithelial cells and renal epithelial cells by examining the effect of occludin protein knockdown or expression of mutant occludin protein on paracellular permeability parameters [Balda et al., 1996; Yu et al., 2005; Al-Sadi et al., 2011; Buschmann et al., 2013]. To date, the role of occludin protein in mediating the effect of different stimuli/manipulations on paracellular permeability is less well-defined. The ability of Tumor Necrosis Factor- $\alpha$  and interferon- $\gamma$  to increase epithelial cell paracellular permeability required occludin protein expression in both intestinal epithelial cells [Buschmann et al., 2013] and renal epithelial cells [Van Itallie et al., 2010]. In contrast, modulation of renal epithelial cell paracellular permeability by src family kinase inhibitors was not dependent on the presence of occludin protein [Caswell et al., 2013]. These studies suggest that the role of occludin protein in mediating the effect of a stimulus on epithelial cell paracellular permeability may be dependent on both the specific stimulus and the specific cell type.

Breakdown of the renal paracellular permeability barrier contributes to pathogenesis of a number of disease states, such as renal ischemia/reperfusion injury [Kwon et al., 1998] and radiocontrast nephropathy [Cheung et al., 2008]. These disease states are associated with an increase in the renal tissue content of hydrogen peroxide,  $H_2O_2$  [Haeussler et al., 2004; Devarajan, 2005]. Exposure of MDCK cell monolayers (a distal tubule-like renal epithelial cell line) to  $H_2O_2$  increased paracellular permeability to small ions and/or large solutes [Meyer et al., 2001; Gonzalez et al., 2009; Yu et al., 2012], indicating that renal epithelial cells in culture may provide a model system in which to study the molecular events mediating the  $H_2O_2$ -induced increase in renal epithelial paracellular permeability. To date, changes in occludin protein content and/or subcellular localization have been correlated with the  $H_2O_2$ -induced increase in MDCK cell paracellular permeability [Meyer et al., 2001; Gonzalez et al., 2009; Yu et al., 2012] but a cause-effect relationship between occludin protein content and  $H_2O_2$ -induced changes in renal epithelial cell paracellular permeability has not been definitively demonstrated.

In the present study, we have tested directly the role of occludin protein in mediating the  $H_2O_2$ -induced increase in paracellular permeability of renal epithelial cells. The results demonstrate: (1)  $H_2O_2$  treatment of renal epithelial cell monolayers at non-toxic concentrations increased the paracellular permeability to large solutes (leak pathway) without affecting the Transepithelial Resistance (TER) which usually reflects primarily the movement of small ions through the pore pathway; (2) Occludin protein knockdown enhanced the sensitivity and occludin overexpression diminished the sensitivity of MDCK

cell monolayers to H<sub>2</sub>O<sub>2</sub>-induced changes in paracellular permeability; (3) H<sub>2</sub>O<sub>2</sub> at concentrations that produced changes in paracellular permeability did not dramatically alter occludin protein content, distribution between detergent-soluble and -insoluble pools, or subcellular localization; (4) H<sub>2</sub>O<sub>2</sub> treatment slowed the movement of GFP-occludin protein into the tight junction region without affecting the mobility of GFP-occludin protein outside of the tight junction region; and (5) This H<sub>2</sub>O<sub>2</sub>-induced slowing of GFP-occludin movement into the tight junction region was lost when the C-terminal region of occludin protein was deleted.

## MATERIALS AND METHODS

### REAGENTS

Antibodies for immunodetection were obtained from Life Technologies. The antibodies used in this study were: occludin C-terminal rabbit antibody (Cat. Number 404700), occludin rabbit antibody (Cat. Number 71-1500), horseradish peroxidase-conjugated goat anti-rabbit antibody (Cat. Number A-10547), and Alexa488-conjugated goat anti-rabbit antibody (Cat. Number A-11034). Rhodamine-Phalloidin was obtained from Life Technologies (Cat. Number A-12381).

### CELL CULTURE

Stock cultures of renal epithelial cell lines (LLC-PK<sub>1</sub>/Cl4, MDCK, MDCK-occludin knockdown, and MDCK-occludin overexpressing) were maintained at a subconfluent density as described previously [Caswell et al., 2013]. All of the MDCK cell lines used in this study are Type II MDCK cell lines (low resistance). The parental MDCK cell line, MDCK-occludin knockdown cell line and MDCK-occludin over-expressing cell line were a gift from Dr. C. Van Itallie (NIHLB) and Dr. E.E. Schneeberger (Massachusetts General Hospital and Harvard Medical School). All MDCK cell lines were derived from the same parental MDCK cell line. The development and characterization of the occludin knockdown cell line is described in Yu et al. [2005]. The development and characterization of the occludin overexpressing cell line is described in Medina et al. [2000] and Van Itallie et al. [2010]. The LLC-PK<sub>1</sub>/Cl4 cell line used in these studies is a random subclone of the original LLC-PK<sub>1</sub> cell strain [Amsler and Cook, 1985]. Cell cultures were checked for mycoplasma contamination upon thaw of a new stock vial and periodically thereafter (MycoAlert Mycoplasma Detection Kit, Lonza). All tests were uniformly negative. New stock cell populations were thawed after 15 passages.

Trypan Blue-exclusion of cell populations following 5 h treatment without or with H<sub>2</sub>O<sub>2</sub> was performed as described previously [Caswell et al., 2013]. TUNEL assay was performed according to manufacturer's instructions (Life Technologies). WST-1 assay was performed according to manufacturer's instructions (Abcam).

### PARACELLULAR PERMEABILITY

The paracellular permeability of renal epithelial cell monolayers to large solutes was determined using calcein as the solute and to small ions was determined by measuring TER as previously described [Caswell et al., 2013].

## WESTERN BLOT ANALYSIS

Cell lysates were prepared from cell populations maintained under the same conditions as used for the measurement of paracellular permeability. Following 2 h treatment with varying concentrations of H<sub>2</sub>O<sub>2</sub>, a time point at which permeability was increased, lysates of total cell protein and Triton X-100-soluble and -insoluble fractions were prepared as previously described [Caswell et al., 2013]. Western blotting was performed as previously described [Caswell et al., 2013]. Occludin antibodies were used at a dilution range of 1:100–1:500. HRP-conjugated anti-rabbit antibody was used at a dilution of 1:10,000.

## IMMUNOFLUORESCENCE MICROSCOPY

Cell populations grown on permeable membrane filters were treated without or with 55 μM H<sub>2</sub>O<sub>2</sub> for 2 h and then fixed with 4% paraformaldehyde and processed for immunofluorescence microscopy as described previously [Caswell et al., 2013]. Cells were labelled either with occludin antibody followed by Alexa488-conjugated secondary antibody or with rhodamine-phalloidin. Occludin antibodies were used at a dilution range of 1:10–1:50. Alexa488-conjugated rabbit antibody was used at a dilution range of 1:100–1:500. Presented images are representative of at least three images obtained from at least two independent samples.

## IMAGE ANALYSIS

Images were acquired and analyzed as described previously [Caswell et al., 2013].

## ADENOVIRAL CONSTRUCT CLONING

Polymerase chain reaction (PCR) was employed to amplify full length hOccludin and a C-terminal truncated hOccludin from the EGFP-hOccludin construct (a gift from Dr. J.R. Turner) and to introduce restriction sites (KpnI and XbaI) using the following primers:

Full-Length hOccludin primers (1,500 bp)—Forward: TACAAGT-  
CCGACTCAGATCTCGAGCTCAAGCTTCGAATTCTGCAGTCGACG-  
GTACCATGTCATCCAGGCCTCTGA

Reverse: TGATCAGTTATCTAGATCCGGTGGATCCCGGGCCCGC-  
GGATAAATGTGTTCCCTTGCCCA

C-Terminal Truncated hOccludin primers (860 bp)—Forward:  
TACAAGTCCGACTCAGATCTCGAGCTCAAGCTTCGAATTCTGCA-  
GTCGACGGTACCATGTCATCCAGGCCTCTGA

Reverse: ACTAGATCTAGAGGTACCGGATCCTGTTTTCTGTCTAT-CATAGT

hOccludin constructs were ligated into the pAcGFP1-Hyg-C1 vector and expanded by transformation into DH5α cells. The full-length hOccludin-EGFP and the C-terminal truncated-hOccludin-EGFP coding sequences were isolated using and KpnI and XbaI restriction sites and were amplified by PCR using the following primers:

Full-Length hOccludin primers (2,500 bp)—Forward: AGATCTC-GAGCTCAAGCTTCTGAATTCTGCAGTCGACGGTACCATGGTGAGCA-AGGGCGAGGAGCTG

Reverse: TGATCAGTTATCTAGATCCGGTGGATCCCGGGCCCCG-GGATAAATGTGTTTCCTTGTCCCA

C-Terminal Truncated EGFP-hOccludin primers (1,500 bp)—Forward: AGATCTCGAGCTCAAGCTTCTGAATTCTGCAGTCGACGG-TACCATGGTGAGCAAGGGCGAGGAGCTG

Reverse: ACTAGATCTAGAGGTACCGGATCCTGTTTTCTGTCTAT-CATAGT

Full-length hOccludin-EGFP and C-terminal truncated hOccludin-EGFP coding sequences were obtained using the KpnI and XbaI restriction sites and were cloned into the pAdEasy-1 adenoviral vector according to the manufacturer's instructions (Agilent Technologies, catalog# 240010-12).

## FLUORESCENCE RECOVERY AFTER PHOTBLEACHING

Cell populations were seeded onto sterile 18 mm round cover glass pieces and placed in sterile 35 mm petri dishes. Cell populations were grown to and maintained at confluence for at least 7 days. Cell populations were transduced with an adenovirus containing full-length EGFP-hOccludin construct (pAdenovirus-hOccludin-FL-EGFP) at a 50:1 MOI. Transduced cells were serum starved overnight ( $\alpha$ MEM, 2 mM L-glutamine, penicillin/streptomycin). FRAP experiments were performed 3–6 days after viral transduction. Transduced cell populations were treated with Ca-Mg-containing PBS  $\pm$  55  $\mu$ M H<sub>2</sub>O<sub>2</sub> for 2 hr at 37°C. Cells were then analyzed by FRAP. Cover slips containing cell populations were mounted onto a chamber and incubated in Ca-Mg-PBS maintained at 37°C. Cells were imaged using a Leica TCS SP5 inverted microscope with 63.0  $\times$  NA 1.40 oil-immersion objective. Data were collected and processed using Leica Microsystems LAS AF software. The tight junction region or a non-tight junction region of the apical membrane was selected for FRAP. The settings for the FRAP procedure were: Argon laser power = 5%; Leica-488 nm laser power = 5%–10%; pre-bleach—5 frames per 1.318 s; bleach—5 frames; post-bleach—1–5 frames per 1.318 s; post-bleach—2–20 frames per 5 s; post-bleach—3–40 frames per 10 s.

## STATISTICAL ANALYSIS

Unless otherwise indicated, data are presented as mean  $\pm$  standard deviation of at least three independent samples. Significance of difference between multiple groups was determined by one way ANOVA with subsequent contrast analysis using a *t*-test. Significance of difference between 2 samples was determined by one-tailed or two-tailed *t*-test. If data failed the Normality test, comparison of control and treated groups was performed by the Mann–Whitney U test. Significance was defined as  $P < 0.05$ .

## RESULTS

### HYDROGEN PEROXIDE TREATMENT INCREASES CALCEIN TRANSEPITHELIAL FLUX

The rate of calcein movement, a “leak” pathway marker [Caswell et al., 2013], across MDCK cell monolayers was increased by pretreatment of cell monolayers with hydrogen peroxide ( $\text{H}_2\text{O}_2$ ) (Fig. 1a). There was no effect of 22  $\mu\text{M}$   $\text{H}_2\text{O}_2$  but a statistically significant concentration-dependent increase in the movement of calcein was observed in MDCK cell monolayers treated with 44  $\mu\text{M}$   $\text{H}_2\text{O}_2$  and above ( $P < 0.01$  compared to 0  $\mu\text{M}$   $\text{H}_2\text{O}_2$  calcein flux). A statistically significant  $\text{H}_2\text{O}_2$  concentration-dependent increase in paracellular calcein flux was also observed with LLC-PK<sub>1</sub> cells at  $\text{H}_2\text{O}_2$  concentrations above 50  $\mu\text{M}$  (Fig. 1b;  $P < 0.01$ ). Treatment of MDCK or LLC-PK<sub>1</sub> cell monolayers with  $\text{H}_2\text{O}_2$  in the same concentration range did not alter significantly TER (Fig. 1c). Treatment of MDCK or LLC-PK<sub>1</sub> cell monolayers with  $\text{H}_2\text{O}_2$  in this concentration range for 5 h, the length of the pretreatment plus flux assay period, did not increase the number of Trypan Blue-positive cells in the cell populations (Fig. 1d). There was no significant increase in staining with the TUNEL assay (data not shown) or the WST-1 assay (data not shown). As expected, markedly higher  $\text{H}_2\text{O}_2$  concentrations were toxic to both MDCK cells and LLC-PK<sub>1</sub> cells (data not shown). Thus, at low concentrations,  $\text{H}_2\text{O}_2$  treatment of renal epithelial cell monolayers increased paracellular permeability via the “leak” pathway.

### OCCLUDIN PROTEIN CONTENT MODULATES THE ABILITY OF $\text{H}_2\text{O}_2$ TO INCREASE “LEAK” PATHWAY PERMEABILITY

Previous work has implicated occludin protein in mediating the ability of cytokines to modulate paracellular permeability [Van Itallie et al., 2010], although occludin protein was not always required to modulate paracellular permeability [Caswell et al., 2013]. To assess the involvement of occludin protein in mediating the  $\text{H}_2\text{O}_2$ -induced enhancement of “leak” pathway permeability, the response to  $\text{H}_2\text{O}_2$  was compared in wild type MDCK cell monolayers and in monolayers of MDCK cells in which occludin protein was either over-expressed or knocked-down. Measurement of the effect of varying  $\text{H}_2\text{O}_2$  concentrations on calcein flux across the three cell lines was performed in a single experiment to ensure that the cell lines were examined under identical conditions. As shown above,  $\text{H}_2\text{O}_2$  treatment of wild type MDCK cell monolayers produced a concentration-dependent enhancement of calcein paracellular flux (Fig. 2a). In monolayers of MDCK cells overexpressing occludin, the response to  $\text{H}_2\text{O}_2$  was substantially attenuated (Fig. 2b). Conversely, in monolayers of MDCK cells in which occludin protein expression was knocked-down, the response to  $\text{H}_2\text{O}_2$  was markedly increased (Fig. 2c). To visualize the relative effect of different  $\text{H}_2\text{O}_2$  concentrations on calcein flux in the different MDCK cell lines, the fold change in calcein flux rate for each  $\text{H}_2\text{O}_2$  concentration compared to 0  $\mu\text{M}$   $\text{H}_2\text{O}_2$  was calculated for each cell line (Fig. 2d). The statistical significance of the difference between the responsiveness of either the occludin overexpressing or the occludin knockdown MDCK cell line compared to the wild type MDCK cell line was confirmed using two different approaches, i.e., by comparing calcein flux curves as a function of  $\text{H}_2\text{O}_2$  concentration and cell line ( $P < 0.001$  for all comparisons) or by comparing the amount of calcein in the apical chamber for each flux time point as a function of  $\text{H}_2\text{O}_2$  concentration and cell line ( $P < 0.05$  for all time points beyond 30 min).  $\text{H}_2\text{O}_2$  treatment did not alter the TER of any of the cell lines (Fig. 2e). In



our hands, occludin protein knockdown did produce a small but statistically significant decrease in TER compared to wild type MDCK cells and occludin protein overexpressing MDCK cells (wild type MDCK –  $69 \pm 7 \Omega\text{-cm}^2$  ( $n = 12$ ), occludin overexpressing MDCK –  $70 \pm 10 \Omega\text{-cm}^2$  ( $n = 12$ ;  $P > 0.86$  versus wild type MDCK), occludin knockdown MDCK –  $50 \pm 6 \Omega\text{-cm}^2$  ( $n = 12$ ;  $P < 0.001$  versus wild type MDCK)). The expected occludin protein content in the three cell lines was confirmed by Western blot analysis (see Caswell et al., 2013).  $\text{H}_2\text{O}_2$  at the concentrations used in these experiments did not produce a statistically significant increase in cell death in any of the MDCK cell lines ( $P > 0.1$  compared to  $0 \mu\text{M}$   $\text{H}_2\text{O}_2$  for wild type MDCK cells and occludin overexpressing MDCK cells; data not shown). For occludin knockdown MDCK cells, there was also no significant increase in cell death although in cell populations treated with  $66 \mu\text{M}$   $\text{H}_2\text{O}_2$  there was a non-significant trend towards a small increase in cell death ( $P > 0.1$  for  $44 \mu\text{M}$  and  $55 \mu\text{M}$   $\text{H}_2\text{O}_2$  and  $P = 0.07$  for  $66 \mu\text{M}$   $\text{H}_2\text{O}_2$ ; data not shown). These results are consistent with our observation that  $\text{H}_2\text{O}_2$ -induced cytotoxicity in renal epithelial cells is typically observed near to or above  $70 \mu\text{M}$   $\text{H}_2\text{O}_2$ .

### **$\text{H}_2\text{O}_2$ DOES NOT DRAMATICALLY ALTER OCCLUDIN PROTEIN CONTENT OR DISTRIBUTION**

Previous studies have reported that occludin protein content and/or localization was altered by treatment of epithelial cells with compounds that increase paracellular permeability, including with  $\text{H}_2\text{O}_2$  [Basuroy et al., 2003; Watson et al., 2005; Gonzalez et al., 2009]. We, therefore, examined whether or not treatment with  $\text{H}_2\text{O}_2$  at the concentrations that increase “leak” pathway permeability also produced changes in occludin protein content and/or localization. First, the effect of  $\text{H}_2\text{O}_2$  treatment on total occludin protein content and content in the Triton X-100-soluble fraction versus the Triton X-100-insoluble fraction were examined. Treatment of MDCK cell monolayers with  $55 \mu\text{M}$   $\text{H}_2\text{O}_2$  for 2 h, a time point at which the change in “leak” pathway permeability is observed, did not alter significantly the occludin protein content in the total cell lysate, the Triton X-100-soluble fraction, or the Triton X-100-insoluble fraction (Fig. 3). The presence of 3 bands in the total cell lysate but not in either the Triton X-100-soluble or -insoluble lysates was not a consistent observation. The intensity of each band in the total cell lysate was not, however, altered by  $\text{H}_2\text{O}_2$  treatment. Equal amounts of cell lysate protein were loaded in each lane, as confirmed by the equal signal strength for ERK 1/2 protein content in each lane (Fig. 3).

To assess the possibility that  $\text{H}_2\text{O}_2$  treatment altered the subcellular distribution of occludin protein, occludin protein was localized by immunofluorescence confocal microscopy in untreated MDCK cells and in MDCK cells treated with  $55 \mu\text{M}$   $\text{H}_2\text{O}_2$  for 2 h (Fig. 4–Occludin). The cell images were divided into thirds along the Z axis to yield an apical section, a middle section, and a basal section. In untreated MDCK cell monolayers ( $0 \mu\text{M}$   $\text{H}_2\text{O}_2$ ), occludin protein staining in the apical section was most prominent as a continuous line surrounding each cell, consistent with localization of occludin protein to the tight junction region of every cell in the monolayer (Fig. 4–Occludin/ $0 \mu\text{M}$   $\text{H}_2\text{O}_2$ ). The intracellular nuclear staining observed in these immunofluorescence images may reflect the previously reported presence of nuclear occludin [Runkle et al., 2011] or may be non-specific. In either case, the nuclear occludin staining was not demonstrably affected by

treatment with H<sub>2</sub>O<sub>2</sub>. In the middle section, the occludin protein was also detected as a continuous line surrounding each cell. Somewhat brighter staining puncta within the continuous line were observed at many tricellular/multicellular junctions. Little occludin protein was detected in the basal region of the cells except for the nuclear staining. A similar pattern of occludin protein staining in each section was observed in the cell populations treated with 55 μM H<sub>2</sub>O<sub>2</sub> with two differences. First, the intensity of the linear staining appeared somewhat weaker in the 55 μM H<sub>2</sub>O<sub>2</sub>-treated cell populations (Fig. 4–Occludin/55 μM H<sub>2</sub>O<sub>2</sub>) compared to the control cell populations. This was most evident when comparing occludin staining in the middle sections. Second, the relative staining intensity of the puncta at the tricellular/multicellular junctions compared to the bicellular linear staining intensity appeared to be somewhat stronger in the H<sub>2</sub>O<sub>2</sub>-treated cell populations compared to control cell populations.

Since the tight junction is connected to the F-actin cytoskeleton, we compared the occludin protein localization to that of F-actin using rhodamine-phalloidin (Fig. 4–F-Actin). In untreated cell populations, F-actin staining in the apical section exhibited a velveteen appearance along the apical surface of each cell, typical of the staining of the F-actin cores of apical microvilli (F-Actin/0 μM H<sub>2</sub>O<sub>2</sub>). A somewhat brighter linear staining surrounded each cell. The central dark area observed on some cells likely represents the location of the central cilium. The primary staining in the middle section was a broad linear staining surrounding each cell consistent with the cortical actin ring. The basal section exhibited streaks of staining consistent with basally-oriented stress fibers. F-Actin staining in the 55 μM H<sub>2</sub>O<sub>2</sub>-treated cell populations was similar in all sections. A modest decrease in stress fiber density was often, but not always observed.

Merging the occludin protein and F-actin images for each section (Fig. 4–Merge) reveals two differences between the untreated and 55 μM H<sub>2</sub>O<sub>2</sub>-treated populations that are most evident in the middle sections. First, the colocalization of occludin protein and F-actin at the tight junction region (yellow color) is more pronounced in the untreated cell populations than in the 55 μM H<sub>2</sub>O<sub>2</sub>-treated cell populations. Second, there is a broadening and, perhaps, even splitting of some of the bright puncta of colocalized occludin protein and F-actin staining at the tricellular junctions of the 55 μM H<sub>2</sub>O<sub>2</sub>-treated cell populations (white arrows).

## H<sub>2</sub>O<sub>2</sub> SLOWS THE MOVEMENT OF OCCLUDIN PROTEIN INTO THE TIGHT JUNCTION

Using the FRAP technique, recent work has demonstrated that tight junction proteins, including occludin protein, exhibit dynamic movement into and out of the tight junction region of cultured epithelial cells [Shen et al., 2009; Buschmann et al., 2013; Raleigh et al., 2013]. We examined the effect of H<sub>2</sub>O<sub>2</sub> treatment on the FRAP behavior of occludin protein by expressing full-length GFP-occludin in MDCK cell monolayers. Expression of full-length GFP-occludin protein was confirmed by Western blot analysis (Fig. 5a) and fluorescence microscopy (Fig. 5b). In untreated MDCK cell monolayers expressing GFP-occludin, photobleaching of a region of the tight junction was followed by a progressive recovery of GFP fluorescence into the photobleached area (Fig. 5b). Analysis of the fluorescence recovery curve for the photobleached area (Fig. 5c) yields the two parameters,



the  $t_{1/2}$  (the time to recover 50% of the maximal recovered fluorescence) and the Percent Immobile Fraction (the percentage of expressed GFP-occludin that is not free to move). For the presented experiment on untreated MDCK cells (Fig. 5c – 0  $\mu\text{M}$   $\text{H}_2\text{O}_2$ ), these values are  $t_{1/2} = 42.54$  s and Percent Immobile Fraction = 35%. The FRAP procedure was performed on multiple replicates of untreated MDCK cell monolayers and results were compared to fluorescence recovery in multiple replicates of MDCK cell monolayers treated with 55  $\mu\text{M}$   $\text{H}_2\text{O}_2$  for 2 h (Fig. 5c – 55  $\mu\text{M}$   $\text{H}_2\text{O}_2$ ). The  $t_{1/2}$  for the presented trace of MDCK cells treated with 55  $\mu\text{M}$   $\text{H}_2\text{O}_2$  is 77.8 s and the Percent Immobile Fraction is 39%. The average values obtained from the multiple replicates are shown in Table I. Compared to untreated MDCK cell monolayers, treatment with  $\text{H}_2\text{O}_2$  increased significantly the  $t_{1/2}$  for GFP-occludin fluorescence recovery into the tight junction region without affecting significantly the Percent Immobile Fraction. Higher  $\text{H}_2\text{O}_2$  concentrations produced progressively greater increases in the  $t_{1/2}$  without affecting the Percent Immobile Fraction significantly (data not shown).

To determine if this effect of  $\text{H}_2\text{O}_2$  was due to a general perturbation of membrane protein mobility, we examined the FRAP behavior for GFP-occludin protein present on the apical membrane, away from the tight junction region, in untreated and 55  $\mu\text{M}$   $\text{H}_2\text{O}_2$ -treated MDCK cell monolayers. Representative traces of fluorescence recovery of full-length GFP-occludin within the apical membrane of untreated and  $\text{H}_2\text{O}_2$ -treated MDCK cell monolayers are shown (Fig. 5d). The data indicate that treatment with  $\text{H}_2\text{O}_2$  had no significant effect on either the  $t_{1/2}$  or the Percent Immobile Fraction for full-length GFP-occludin protein expressed on the apical membrane (Table II). Even at higher  $\text{H}_2\text{O}_2$  concentrations, there was no effect on the  $t_{1/2}$  of GFP-occludin moving within the apical membrane (data not shown). Interestingly, the Percent Immobile Fraction for full-length GFP-occludin moving within the apical membrane was significantly smaller than the Percent Immobile Fraction for full-length GFP-occludin moving into the tight junction ( $P < 0.001$ ). These results argue that the observed effect of  $\text{H}_2\text{O}_2$  on full-length GFP-occludin  $t_{1/2}$  is specific for movement of GFP-occludin into the tight junction region.

The occludin protein C-terminal tail region contains multiple interaction domains and potential phosphorylation sites that may be important in the regulation of paracellular permeability (for reviews, see Feldman et al., 2005; Rao, 2009; Cummins, 2012). To determine if this region is required for the observed  $\text{H}_2\text{O}_2$ -dependent slowing of full-length GFP-occludin movement into the tight junction region, we constructed a mutant GFP-occludin protein in which the entire C-terminal region was deleted. Expression of C-terminal truncated GFP-occludin protein was confirmed by Western blot analysis (Fig. 5a) and fluorescence microscopy (data not shown). The ability of  $\text{H}_2\text{O}_2$  to slow the dynamic movement of this mutant GFP-occludin protein into the tight junction region was assessed. In contrast to the slowing of full-length GFP-occludin protein,  $\text{H}_2\text{O}_2$  treatment for 2 hr had no significant effect on either the  $t_{1/2}$  or Percent Immobile Fraction of the C-terminal truncated GFP-occludin protein (Table I). Representative traces of fluorescence recovery for C-terminal truncated GFP-occludin are shown (Fig. 5e). Higher  $\text{H}_2\text{O}_2$  concentrations also did not affect the  $t_{1/2}$  or Percent Immobile Fraction of C-terminal truncated GFP-occludin protein movement into the tight junction (data not shown). The Percent Immobile Fraction

of C-terminal truncated GFP-occludin moving into the tight junction region was significantly smaller than the Percent Immobile Fraction of full-length occludin moving into the tight junction region ( $P < 0.001$ ). The Percent Immobile Fractions for full-length GFP-occludin moving within the apical membrane and for C-terminal truncated GFP-occludin moving into the tight junction region were not significantly different ( $P = 0.285$ ).

## DISCUSSION

Our results confirm previous studies demonstrating that treatment with  $H_2O_2$  increases paracellular permeability of renal epithelial cells [Collares-Buzato et al., 1998; Meyer et al., 2001; Gonzalez et al., 2009; Yu et al., 2012] and other cell types [Rao et al., 1997; Takenaga et al., 2009; Caraballo et al., 2011]. We have demonstrated that  $H_2O_2$  treatment increases leak pathway permeability of renal epithelial cells without markedly affecting pore pathway permeability. Some previous studies examining the effects of  $H_2O_2$  on MDCK renal epithelial cells, one of the renal epithelial cell lines used in our studies, reported parallel increases in permeability via both the leak and pore pathways [Gonzalez et al., 2009; Yu et al., 2012]. Studies from the Rao group report increases in both pore and leak pathway permeability upon treatment of Caco-2 intestinal epithelial cells with  $H_2O_2$  [Rao et al., 2001; Basuroy et al., 2003; Basuroy et al., 2006]. This difference in  $H_2O_2$  effects on the pore versus leak pathways may reflect technical differences between the studies and/or cell type differences in responsiveness to  $H_2O_2$ . For example, multiple differences between renal and intestinal cell regulation of tight junction permeability have been reported [Jepson, 2003; Shen et al., 2011; Caswell et al., 2013; unpublished data].

A role for occludin protein in mediating/regulating paracellular permeability is still controversial. Yu et al. [2010] reported that occludin knockdown did not affect steady state pore pathway permeability of MDCK cells or the permeability of large solutes but did increase permeability of moderate-sized solutes (3.6–7.2Å – a range spanning the shift from pore to leak pathway; Watson et al. [2001]). Van Itallie et al. [2010] reported no effect of occludin knockdown in MDCK cells on either pore or leak pathways. Al-Said et al. [2011] reported that partial knockdown of occludin in Caco-2 intestinal epithelial cells did not affect pore pathway permeability but increased leak pathway permeability. In contrast, Buschmann et al. [2013] reported that more extensive occludin knockdown in Caco-2 cells increased both pore and leak pathway permeability. In our hands, knockdown of occludin protein in MDCK cells did not markedly affect basal leak pathway permeability despite >90% decrease in expression of occludin protein. We did observe a modest but statistically significant increase in pore pathway permeability with occludin protein knockdown.

The focus of this study was to examine the involvement of occludin protein in the  $H_2O_2$ -induced increase in renal epithelial cell paracellular permeability. Our results demonstrate directly that occludin protein content affects the sensitivity of MDCK cell paracellular permeability to  $H_2O_2$ . This is in contrast to the lack of effect of manipulation of occludin protein content on the ability of src Family Kinase inhibitors to increase renal epithelial cell paracellular permeability [Caswell et al., 2013]. Many previous studies using a variety of epithelial cell types have correlated changes in occludin protein content and/or subcellular localization with changes in paracellular permeability produced by different stimuli [Rao et

al., 2001; Bruewer et al., 2004; Sabath et al., 2008; Gonzalez et al., 2009; Caraballo et al., 2011; Yu et al., 2012]. We were unable to detect a marked change in either occludin protein content or occludin protein distribution between detergent-soluble and -insoluble fractions. This suggests that a major change in occludin protein organization state is not necessary to produce a change in paracellular permeability, at least via the leak pathway.

In this study, we demonstrate that H<sub>2</sub>O<sub>2</sub>-induced changes in paracellular permeability of renal epithelial cells were correlated with changes in the rate of lateral movement of occludin protein into the tight junction region. This effect of H<sub>2</sub>O<sub>2</sub> was concentration dependent, was not observed for GFP-occludin protein movement into areas outside of the tight junction, and required the cytoplasmic C-terminal tail region of occludin protein. Shen et al. [2009] first demonstrated that tight junction proteins, including occludin protein, exhibited dynamic movement into and out of the tight junction region of MDCK cells. The shorter half-time for recovery of GFP-occludin fluorescence into the tight junction region measured in our study (~50 s) compared to that reported by Shen et al. [2009; ~200 s] is consistent with their finding that the measured  $t_{1/2}$  decreased with the length of time the cells were maintained at confluence.

Our studies indicate that H<sub>2</sub>O<sub>2</sub> treatment of MDCK cell monolayers slowed the movement of GFP-occludin protein into the tight junction region, increasing the  $t_{1/2}$  from ~50 s (control) to ~80 s (55  $\mu$ M H<sub>2</sub>O<sub>2</sub>). Treatment with 110  $\mu$ M H<sub>2</sub>O<sub>2</sub> increased the  $t_{1/2}$  further (data not shown). Treatment of Caco-2<sub>BBE</sub> cell monolayers with tumor necrosis factor (TNF), which increases paracellular permeability of Caco-2<sub>BBE</sub> cells, accelerated the movement of GFP-occludin into the tight junction [Buschmann et al., 2013]. This was correlated with a dissociation of GFP-occludin protein from the tight junction region following TNF treatment. Raleigh et al. [2013] reported that inhibition of CK2-dependent phosphorylation of occludin protein on S408 in Caco-2<sub>BBE</sub> cells increased TER and, in parallel, decreased the occludin protein mobile fraction without altering the  $t_{1/2}$  for occludin protein. Thus, increased paracellular permeability can be associated with either an increased or a decreased mobility of occludin protein into the tight junction. While seemingly at odds, these results may be reconciled by the possibility that changes in steady state conditions of the tight junction, either by increasing or decreasing occludin protein mobility into the junction, could disrupt junctional integrity leading to increased paracellular permeability. Alternatively, the different results obtained with Caco-2<sub>BBE</sub> (intestinal) versus MDCK (renal) cells could reflect cell type-specific differences in tight junction regulation, as have been reported previously [see, e.g., Jepson, 2003; Shen et al., 2011; Caswell et al., 2013]. The lack of H<sub>2</sub>O<sub>2</sub> effect on mobility of GFP-occludin protein in the plane of the apical membrane away from the tight junction indicates that H<sub>2</sub>O<sub>2</sub> is affecting selectively movement of GFP-occludin into the tight junction region, supporting a role for this action in the H<sub>2</sub>O<sub>2</sub>-induced regulation of paracellular permeability. The inability of H<sub>2</sub>O<sub>2</sub> to alter the mobility of C-terminal truncated GFP-occludin protein also supports this hypothesis since the C-terminal region contains multiple interaction and phosphorylation domains implicated in mediating regulation of paracellular permeability [see, e.g., Cummins, 2012; Buschmann et al., 2013; Doerfel et al., 2013; Raleigh et al., 2013].

In our study, the manipulations that eliminated the ability of H<sub>2</sub>O<sub>2</sub> to increase the  $t_{1/2}$  for occludin movement into the tight junction region, C-terminal truncation and movement within the apical membrane, also increased the accessible mobile fraction of occludin protein. The effect of C-terminal truncation on occludin protein mobile fraction is consistent with the findings of Buschmann et al. [2013] who reported a similar increase in occludin protein mobile fraction in intestinal epithelial cells when the OCEL domain, the distal portion of the C-terminal domain from aa 416-522, was deleted. The OCEL domain contains the ZO-1 binding site as well as multiple phosphorylation sites [Feldman et al., 2005; Li et al., 2005; Rao, 2009; Cummins, 2012]. Raleigh et al. [2011] reported that CK2-dependent phosphorylation of occludin on S408 increased the occludin protein mobile fraction and weakened the interaction of occludin with ZO-1. Since three different conditions that weaken or eliminate the interaction of occludin with ZO-1 increase the occludin protein mobile fraction, it is tempting to speculate that the extent of interaction of occludin protein with ZO-1 protein is a significant determinant of the percentage of occludin protein able to move into the tight junction.

## ACKNOWLEDGMENTS

The authors would like to thank the following people for excellent technical assistance: Wai Man, Victoria Rohring, Nikita Shah, Nancy Singh, and Angelina Voronina. The authors would like to thank Dr. C. Van Itallie (NIHLB) and Dr. E.E. Schneeberger (Massachusetts General Hospital and Harvard Medical School) for providing the occludin knockdown and occludin overexpressing MDCK cells lines. The authors would like to thank Dr. Jerrold R. Turner (University of Chicago) for providing the pEGFP-hOccludin construct.

Grant sponsor: NIDDK; Grant number: R15-DK-091749-01A1.

## REFERENCES

- Al-Sadi R, Khatib K, Guo S, Ye D, Youssef M, Ma T. Occludin regulates macromolecule flux across the intestinal epithelial tight junction barrier. *Am J Physiol.* 2011; 300:G1054–G1064.
- Amsler K, Cook JS. Linear relationship of phlorizin-binding capacity and hexose uptake during differentiation in a clone of LLC-PK<sub>1</sub> cells. *J Cell Physiol.* 1985; 122:254–258. [PubMed: 2578475]
- Balda MS, Whitney JA, Flores C, Gonzalez S, Cerejido M, Matter K. Functional dissociation of paracellular permeability and transepithelial electrical resistance and disruption of the apical-basolateral intramembrane diffusion barrier by expression of a mutant tight junction membrane protein. *J Cell Biol.* 1996; 134:1031–1049. [PubMed: 8769425]
- Basuroy S, Sheth P, Kuppuswamy D, Balasubramanian S, Ray RM, Rao RK. Expression of kinase-inactive c-src delays oxidative stress-induced disassembly and accelerates calcium-mediated reassembly of tight junctions in the Caco-2 cell monolayer. *J Biol Chem.* 2003; 278:11916–11924. [PubMed: 12547828]
- Basuroy S, Seth A, Elias B, Naren AP, Rao R. MAPK interacts with occludin and mediates EGF-induced prevention of tight junction disruption by hydrogen peroxide. *Biochem J.* 2006; 393:69–77. [PubMed: 16134968]
- Bruwer M, Hopkins AM, Hobert ME, Nusrat A, Madara JL. RhoA, Rac1, and Cdc42 exert distinct effects on epithelial barrier via selective structural and biochemical modulation of junctional proteins and F-actin. *Am J Physiol.* 2004; 287:C327–C335.
- Buschmann MM, Shen L, Rajapakse H, Raleigh DR, Wang Y, Wang Y, Lingaraju A, Zha J, Abbott E, McAuley EM, Breskin LA, Wu L, Anderson K, Turner JR, Weber CR. Occludin OCEL-domain interactions are required for maintenance and regulation of the tight junction barrier to macromolecular flux *Molec Biol Cell.* 2013; 24:3056–3068. [PubMed: 23924897]

- Caraballo JC, Yshii C, Butti ML, Westphal W, Borcherding JA, Allamargot C, Comellas AP. Hypoxia increases transepithelial electrical conductance and reduces occludin at the plasma membrane in alveolar epithelial cells via PKC-z and PP2A pathway. *Am J Physiol.* 2011; 300:L569–L578.
- Caswell D, Jaggi S, Axis J, Amsler K. src Family kinases regulate renal epithelial paracellular permeability through an occludin-independent mechanism. *J Cell Physiol.* 2013; 228:1210–1220. [PubMed: 23129414]
- Cheung CM, Ponnusamy A, Anderton JG. Management of acute renal failure in the elderly patient: A clinician's guide. *Drugs Aging.* 2008; 25:455–476. [PubMed: 18540687]
- Collares-Buzato CB, Jepson MA, Simmons NL, Hirst BH. Increased tyrosine phosphorylation causes redistribution of adherens junction and tight junction proteins and perturbs paracellular barrier function in MDCK epithelia. *Eur J Cell Biol.* 1998; 76:85–92. [PubMed: 9696347]
- Cummins PM. Occludin: One protein, many forms. *Molec Cell Biol.* 2012; 32:242–250. [PubMed: 22083955]
- Devarajan P. Cellular and molecular derangements in acute tubular necrosis. *Curr Opin Pediatr.* 2005; 17:193–199. [PubMed: 15800411]
- Doerfel MJ, Westphal JK, Bellmann C, Krug SM, Cording J, Mittag S, Tauber R, Fromm M, Blasig IE, Huber O. CK2-dependent phosphorylation of occludin regulates the interaction with ZO-proteins and tight junction integrity. *Cell Commun Signal.* 2013; 11:40. [PubMed: 23758859]
- Feldman GJ, Mullin JM, Ryan MP. Occludin: Structure, function and regulation. *Adv Drug Deliv Rev.* 2005; 57:883–917. [PubMed: 15820558]
- Gonzalez JE, DiGeronimo RJ, Arthur DE, King JM. Remodeling of the tight junction during recovery from exposure to hydrogen peroxide in kidney epithelial cells. *Free Rad Biol Med.* 2009; 47:1561–1569. [PubMed: 19733232]
- Haeussler U, Riedel M, Keller F. Free reactive oxygen species and nephrotoxicity of contrast agents. *Kidney Blood Press Res.* 2004; 27:167–171. [PubMed: 15256812]
- Jepson MA. Disruption of epithelial barrier function by H<sub>2</sub> O<sub>2</sub>: Distinct responses of Caco-2 and Madin-Darby canine kidney (MDCK) strains. *Cell Mol Biol (Noisy-le-grand).* 2003; 49:101–112. [PubMed: 12839341]
- Kwon O, Nelson WJ, Sibley R, Huie P, Scandling JD, Dafoe D, Alfrey E, Myers BD. Backleak, tight junctions, and cell-cell adhesion in postischemic injury to the renal allograft. *J Clin Invest.* 1998; 101:2054–2064. [PubMed: 9593761]
- Li Y, Fanning AS, Anderson JM, Lavie A. Structure of the conserved cytoplasmic C-terminal domain of occludin: Identification of the ZO-1 binding surface. *J Mol Biol.* 2005; 352:151–164. [PubMed: 16081103]
- Medina R, Rahner C, Mitic LL, Anderson JM, Van Itallie CM. Occludin localization at the tight junction requires the second extracellular loop. *J Membr Biol.* 2000; 178:235–247. [PubMed: 11140279]
- Meyer TN, Schwesinger C, Ye J, Denker BM, Nigam SJ. Reassembly of the tight junction after oxidative stress depends on tyrosine kinase activity. *J Biol Chem.* 2001; 278:22048–22055. [PubMed: 11294856]
- Raleigh DR, Boe DM, Yu D, Weber CR, Marchiando AM, Bradford EM, Wang Y, Wu L, Schneeberger EE, Shen L, Turner JR. Occludin S408 phosphorylation regulates tight junction protein interactions and barrier function. *J Cell Biol.* 2011; 193:565–582. [PubMed: 21536752]
- Rao RK, Baker RD, Baker SS, Gupta A, Holycross M. Oxidant-induced disruption of intestinal epithelial barrier function: Role of protein tyrosine phosphorylation. *Am J Physiol.* 1997; 273:G812–G823. [PubMed: 9357822]
- Rao RK, Basuroy S, Rao VU, Karnaky KJ, Gupta A. Tyrosine phosphorylation and dissociation of occludin-ZO-1 and E-cadherin-b-catenin complexes from the cytoskeleton by oxidative stress. *Biochem J.* 2001; 368:471–481. [PubMed: 12169098]
- Rao R. Occludin phosphorylation in regulation of epithelial tight junctions. *Ann NY Acad Sci.* 2009; 1165:62–68. [PubMed: 19538289]
- Runkle EA, Sundstrom JM, Runkle KB, Liu X, Antonetti DA. Occludin localizes to centrosomes and modifies mitotic entry. *J Biol Chem.* 2011; 286:30847–30858. [PubMed: 21757728]

- Sabath E, Negoro H, Beaudry S, Paniagua M, Angelow S, Shah J, Grammatikakis N, Yu ASL, Denker BM. Ga12 regulates protein interactions within the MDCK cell tight junction and inhibits tight-junction assembly. *J Cell Sci.* 2008; 121:814–824. [PubMed: 18285450]
- Shen L, Weber CR, Turner JR. The tight junction protein complex undergoes rapid and continuous molecular remodeling at steady state. *J Cell Biol.* 2009; 181:683–695. [PubMed: 18474622]
- Shen L, Weber CR, Raleigh DR, Yu D, Turner JR. Tight junction pore and leak pathways: A dynamic duo. *Annu Rev Physiol.* 2011; 73:283–309. [PubMed: 20936941]
- Szaszi K, Amoozadeh Y. New insights into functions, regulation, and pathological roles of tight junctions in kidney tubular epithelium. *Internat Rev Cell Molec Biol.* 2014; 308:205–271.
- Takenaga Y, Takagi N, Murotomi K, Tanonaka K, Takeo S. Inhibition of src activity decreases tyrosine phosphorylation of occludin in brain capillaries and attenuates increase in permeability of the blood-brain barrier after transient focal cerebral ischemia. *J Cerebr Blood Flow Metab.* 2009; 29:1099–1108.
- Van Itallie CM, Fanning AS, Holmes J, Anderson JM. Occludin is required for cytokine-induced regulation of tight junction barriers. *J Cell Sci.* 2010; 123:2844–2852. [PubMed: 20663912]
- Watson CJ, Rowland M, Warhurst G. Functional modeling of tight junctions in intestinal cell monolayers using polyethylene glycol oligomers. *Am J Physiol.* 2001; 281:C388–C397.
- Watson CJ, Hoare CJ, Garrod DR, Carlson GL, Warhurst G. Interferon-g selectively increases epithelial permeability to large molecules by activating different populations of paracellular pores. *J Cell Sci.* 2005; 118:5221–5230. [PubMed: 16249235]
- Yu ASL, McCarthy KM, Francis SA, McCormack JM, Lai J, Rogers RA, Lynch RD, Schneeberger EE. Knockdown of occludin expression leads to diverse phenotypic alterations in epithelial cells. *Am J Physiol.* 2005; 288:C1231–C1241.
- Yu D, Marchiando AM, Weber CR, Raleigh DR, Wang Y, Shen L, Turner JR. MLCK-dependent exchange and actin binding region-dependent anchoring of ZO-1 regulate tight junction barrier function. *Proc Natl Acad Sci USA.* 2010; 107:8237–8241. [PubMed: 20404178]
- Yu W, Beaudry S, Negoro H, Boucher I, Tran M, Kong T, Denker BM. H<sub>2</sub>O<sub>2</sub> activates G protein,  $\alpha$ 12 to disrupt the junctional complex and enhance ischemia reperfusion injury. *Proc Natl Acad Sci USA.* 2012; 109:6680–6685. [PubMed: 22493269]



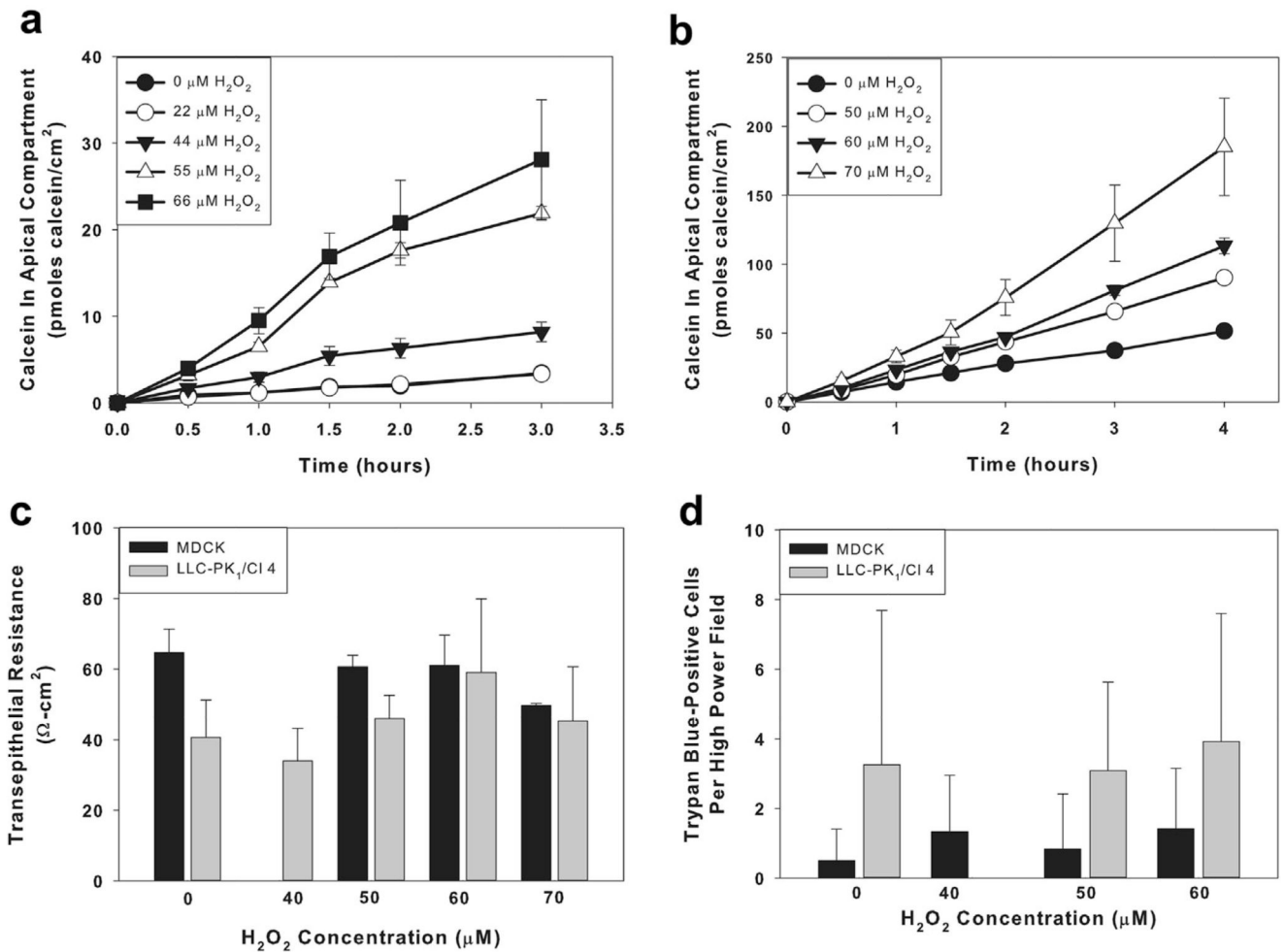


**Fig. 1.** H<sub>2</sub>O<sub>2</sub> increases in a concentration-dependent manner paracellular calcein movement across monolayers of renal epithelial cells. MDCK cell monolayers (a) and LLC-PK<sub>1</sub> cell monolayers (b) were pretreated for 1 h without or with the indicated H<sub>2</sub>O<sub>2</sub> concentration and then calcein movement was measured over the next 4 h in the continued presence of H<sub>2</sub>O<sub>2</sub>. Results are shown as mean ± SD for triplicate independent samples. Data are representative of at least 4 separate experiments. (c) Quantification of the effect of treatment with increasing concentrations of H<sub>2</sub>O<sub>2</sub> for 5 h on transepithelial resistance of MDCK and LLC-PK<sub>1</sub> cell monolayers. Results are shown as mean ± SD of 12 independent measurements. Data are representative of at least four separate experiments. (d) Quantification of the effect of treatment with increasing concentrations of H<sub>2</sub>O<sub>2</sub> for 5 h on Trypan Blue-staining of MDCK cells and LLC-PK<sub>1</sub> cells. Results are shown as mean ± SD of 12 independent measurements. Data are representative of at least four separate experiments.

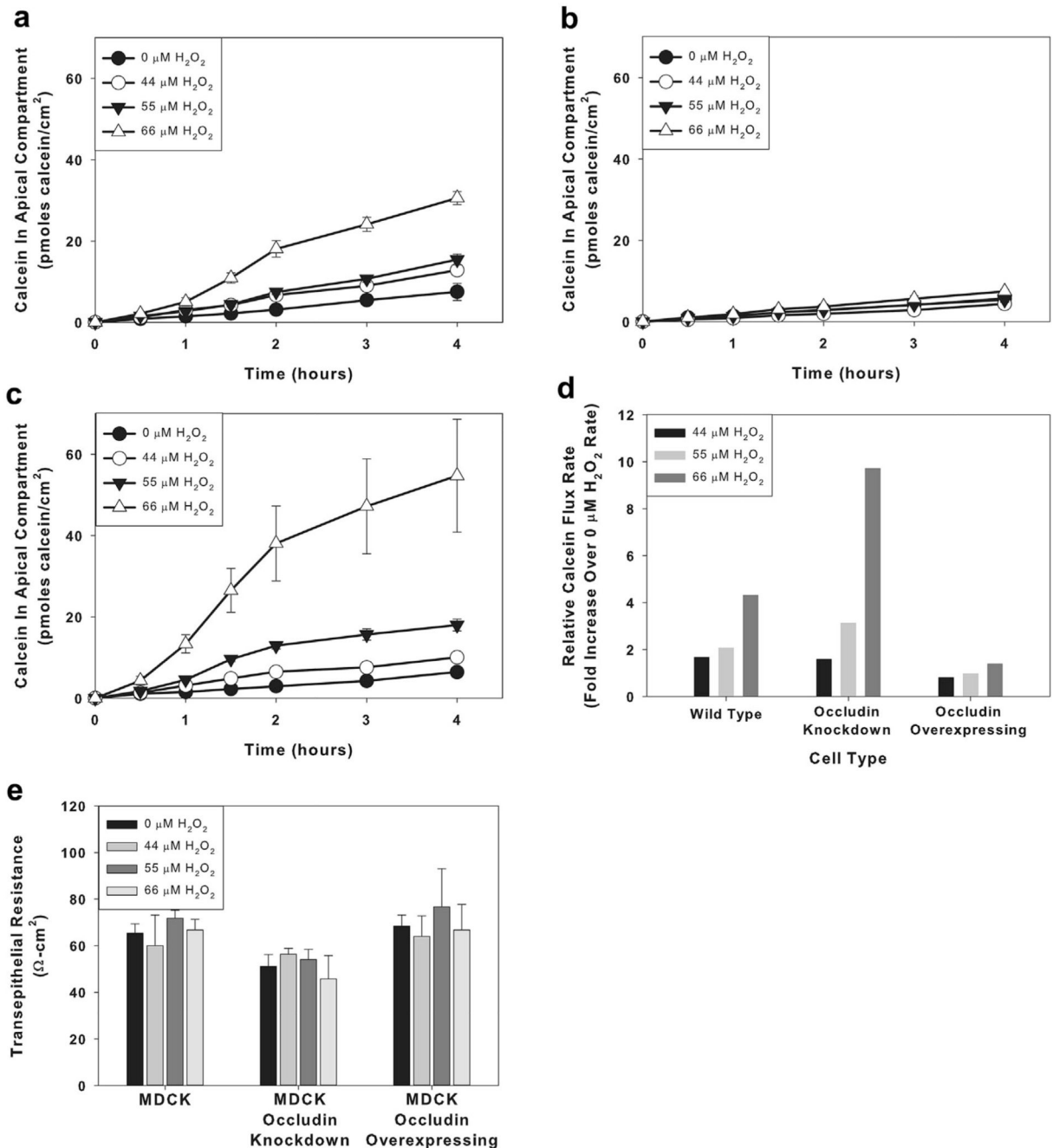


**Fig. 2.** The  $\text{H}_2\text{O}_2$  sensitivity of paracellular calcein flux across MDCK cell monolayers is dependent on occludin protein content. Populations of wild type MDCK cells (a), occludin-overexpressing MDCK cells (b), and occludin knockdown MDCK cells (c) were pretreated for 1 h without or with the indicated  $\text{H}_2\text{O}_2$  concentrations and then calcein movement was measured over the next 4 h in the continued presence of  $\text{H}_2\text{O}_2$ . Results are shown as mean  $\pm$  SD of triplicate independent samples. Data are representative of at least four separate experiments. (d) Fold-change in calcein flux rate at increasing  $\text{H}_2\text{O}_2$  concentrations

compared to the calcein flux rate in untreated cells for wild type MDCK cells, occludin-overexpressing MDCK cells and occludin knockdown MDCK cells. (e) Quantification of the effect of treatment with increasing concentrations of H<sub>2</sub>O<sub>2</sub> for 5 h on transepithelial resistance of wild type MDCK, occludin-overexpressing MDCK, and occludin knockdown MDCK cell monolayers. Results are shown as mean ± SD of 12 independent measurements. Results are representative of at least four separate experiments.

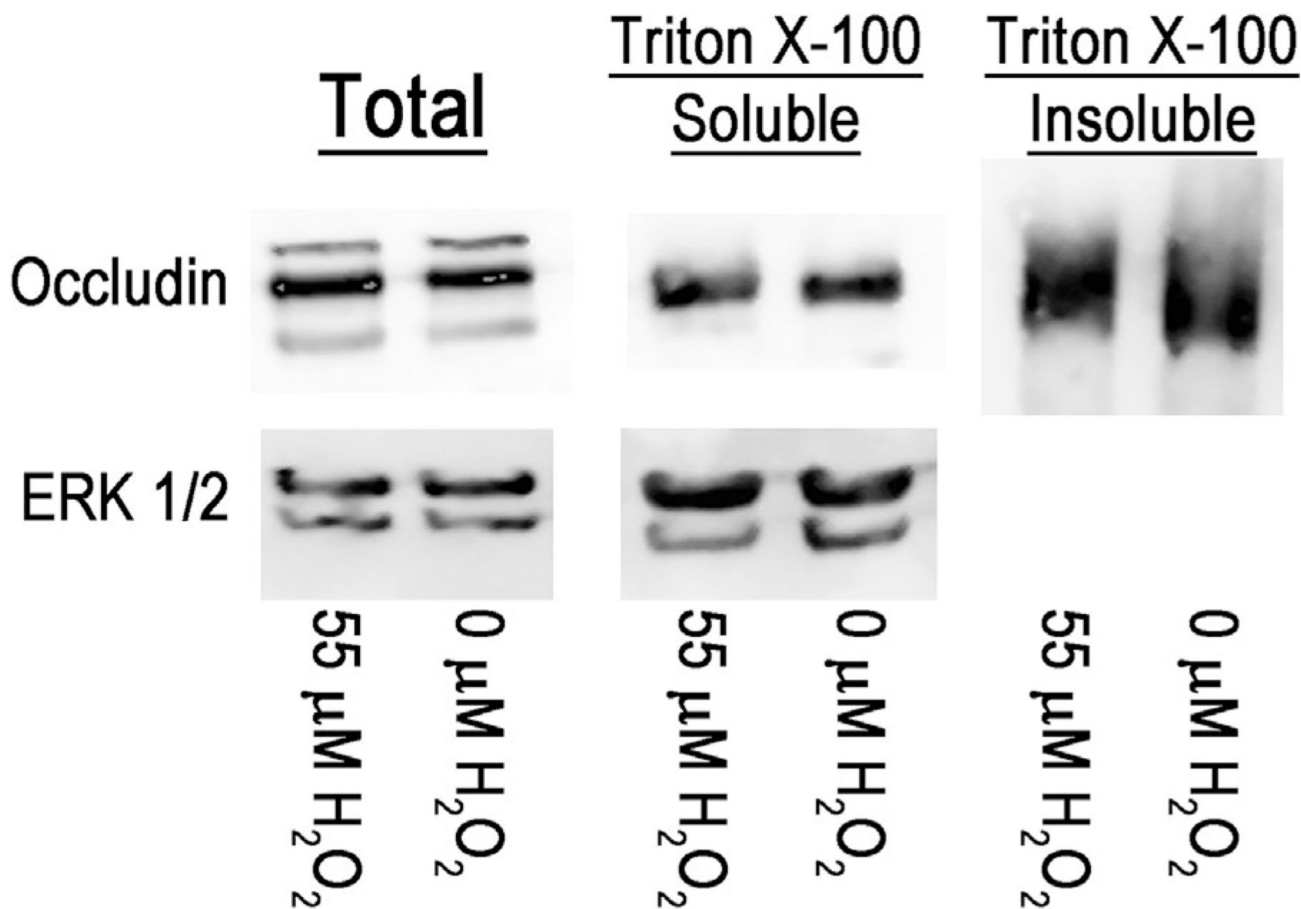


**Fig. 3.** H<sub>2</sub>O<sub>2</sub> treatment does not alter occludin protein content in whole cell lysate, Triton X-100-soluble lysate, or Triton X-100-insoluble lysate. Western blot analysis of the effect of 2 h treatment of MDCK cell monolayers without or with 55 μM H<sub>2</sub>O<sub>2</sub> on occludin protein content in the total cell lysate, the Triton X-100-soluble lysate fraction, and the Triton X-100-insoluble lysate fraction. Western blot analysis of ERK ½ protein content in the total cell lysate and Triton X-100-soluble lysate fraction are shown for comparison.

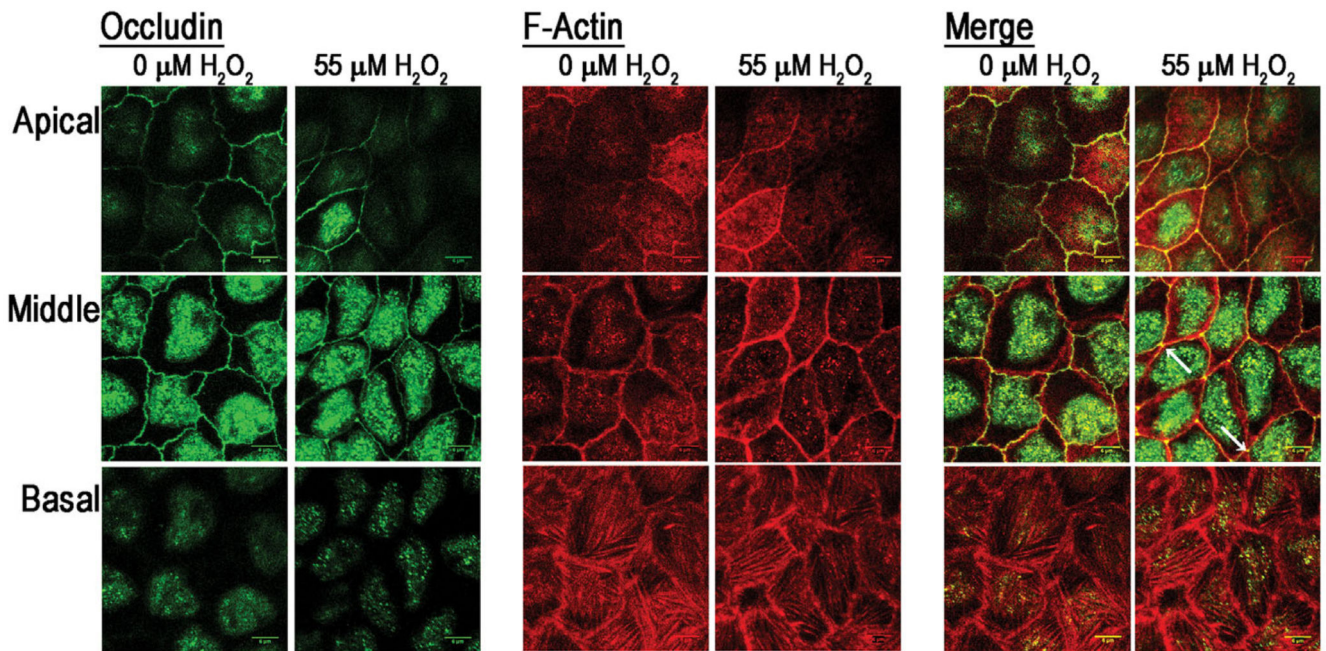


**Fig. 4.**

$\text{H}_2\text{O}_2$  treatment alters occludin colocalization with F-actin at the tight junction region. Confocal images localizing occludin protein and F-actin (rhodamine-phalloidin) in MDCK cell monolayers treated without or with  $55 \mu\text{M H}_2\text{O}_2$  for 2 h. Cell images are divided into three equal sections (apical, middle, and basal) along the Z axis. Note: In middle sections, colocalization of occludin and F-actin along bicellular tight junction regions appears weaker in  $55 \mu\text{M H}_2\text{O}_2$ -treated cell populations. In contrast, colocalization at tricellular tight junctions regions appears relatively stronger in  $55 \mu\text{M H}_2\text{O}_2$ -treated cell populations. Scale bar is located at bottom right of each image. Images are representative of three images from at least two independent experiments.



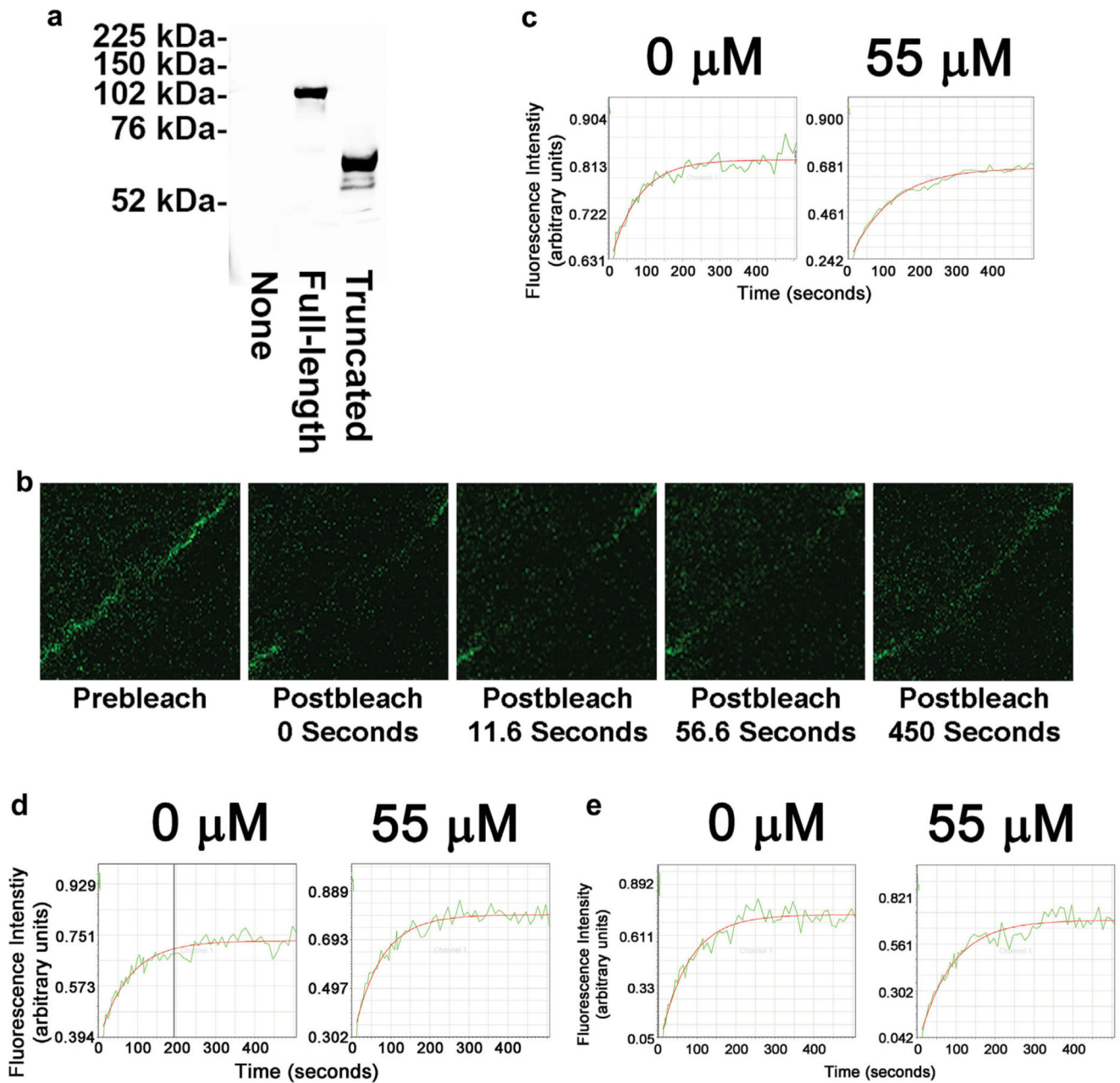


**Fig. 5.**  $\text{H}_2\text{O}_2$  treatment slows the movement of full-length GFP-occludin into the tight junction region but not movement of GFP-occludin within the apical membrane or C-terminal truncated GFP-occludin into the tight junction region. (a) Western blot analysis of expression of GFP-tagged proteins in untransduced MDCK cells (None), MDCK cells transduced with full-length GFP-occludin construct (Full-length) or MDCK cells transduced with C-terminal truncated GFP-occludin construct (Truncated). FRAP analysis was performed on MDCK cell populations transduced with full-length GFP-occludin construct and maintained in the absence or presence of 55  $\mu\text{M}$   $\text{H}_2\text{O}_2$  for 2 h. GFP-occludin in an area of the tight junction region of transduced MDCK cells was photobleached. (b) Images of this



region were obtained prior to, immediately following and at increasing amounts of time following photobleaching. The images shown are obtained from transduced MDCK cells maintained in the absence of H<sub>2</sub>O<sub>2</sub>. (c) The fluorescence signal in the photobleached area was quantitated and plotted as a function of time for transduced MDCK cells treated with 0  $\mu$ M H<sub>2</sub>O<sub>2</sub> or 55  $\mu$ M H<sub>2</sub>O<sub>2</sub>. (d) Representative traces for FRAP analysis of full-length GFP-occludin moving within the apical membrane as a function of time for transduced MDCK cells treated with 0  $\mu$ M or 55  $\mu$ M H<sub>2</sub>O<sub>2</sub>. (e) Representative traces for FRAP analysis of C-terminal truncated GFP-occludin moving into the tight junction region as a function of time for transduced MDCK cells treated with 0  $\mu$ M or 55  $\mu$ M H<sub>2</sub>O<sub>2</sub>.

**TABLE I**

Treatment With H<sub>2</sub>O<sub>2</sub> Slows the Movement of Full-Length GFP-Occludin Protein, but not C-Terminal-Truncated GFP-Occludin Protein Into the Tight Junction Region of Post-Confluent MDCK Cells

	[H <sub>2</sub> O <sub>2</sub> ] (μM)	Recovery halftime (t <sub>1/2</sub> )(s)	Immobile fraction (%)	Number of replicates (n)
Full-length GFP-occludin	0	51.45 ± 10.53	45.7 ± 8.1	10
	55	77.57 ± 10.57**	36.6 ± 13.7	16
Truncated GFP-occludin	0	56.27 ± 18.74	27.2 ± 15.0	42
	55	61.16 ± 18.24	25.3 ± 9.1	37

FRAP analysis was performed on post-confluent MDCK cell populations expressing either full-length GFP-occludin protein or C-terminal-truncated GFP-occludin protein. Prior to FRAP analysis, cell populations were treated without or with 55 μM H<sub>2</sub>O<sub>2</sub> for 2 h. Derived parameters, t<sub>1/2</sub> and % Immobile Fraction, were calculated for each experiment. Results are presented as mean ± SD of derived parameters for the indicated number of independent experiments. Results are representative of studies using at least three separate cell populations.

\*  $P < 0.05$  compared to 0 μM H<sub>2</sub>O<sub>2</sub>

\*\*  $P < 0.01$  compared to 0 μM H<sub>2</sub>O<sub>2</sub>.

**TABLE II**

Treatment With H<sub>2</sub>O<sub>2</sub> Does not Slow the Movement of Full-Length GFP-Occludin Protein Within the Apical Membrane of Post-Confluent MDCK Cells

[H <sub>2</sub> O <sub>2</sub> ] (μM)	Recovery halftime (t <sub>1/2</sub> ) (s)	Immobile fraction (%)	Number of replicates (n)
0	51.68 ± 18.23	28 ± 11	12
55	45.21 ± 21.11	34 ± 17	13

FRAP analysis was performed on post-confluent MDCK cell populations expressing full-length GFP-occludin protein. Prior to FRAP analysis, cell populations were treated without or with 55 μM H<sub>2</sub>O<sub>2</sub> for 2 h. Derived parameters, t<sub>1/2</sub> and % Immobile Fraction, were calculated for each experiment. Results are presented as mean ± SD of derived parameters for the indicated number of independent experiments. Results are representative of studies using at least two separate cell populations.

\*  $P < 0.05$  compared to 0 μM H<sub>2</sub>O<sub>2</sub>

\*\*  $P < 0.01$  compared to 0 μM H<sub>2</sub>O<sub>2</sub>